4-Amino-3-(p-chlorophenyl)-5-(p-methoxybenzyl)-4H-1,2,4-triazole: X-ray and DFT-calculated Structures

Article *in* Chinese Journal of Structural Chemistry · May 2011

CITATIONS
3

READS
39

5 authors, including:

Cihan Kantar
Recep Tayyip Erdoğan Üniversitesi
69 PUBLICATIONS **371** CITATIONS
SEE PROFILE

Olcay Bekircan
Karadeniz Technical University
83 PUBLICATIONS **1,183** CITATIONS
SEE PROFILE

Orhan Büyükgüngör
Ondokuz Mayıs Üniversitesi
1,596 PUBLICATIONS **9,949** CITATIONS
SEE PROFILE

4-Amino-3-(*p*-chlorophenyl)-5-(*p*-methoxybenzyl)-4H-1,2,4-triazole: X-ray and DFT-calculated Structures①

ŞAHİN Onur[a②] KANTAR Cihan[b] BEKİRCAN Olcay[c]
ŞAŞMAZ Selami[b] BÜYÜKGÜNGÖR Orhan[a]
[a] (*Department of Physics, Faculty of Arts and Sciences, Ondokuz Mayıs University, Samsun, Turkey*)
[b] (*Department of Chemistry, Rize University, Rize, Turkey*)
[c] (*Karadeniz Teknik University, Maçka, Turkey*)

ABSTRACT The title compound, 4-amino-3-(*p*-chlorophenyl)-5-(*p*-methoxybenzyl)-4H-1,2,4-triazole **I** , $C_{16}H_{15}ClN_4O$), has been determined using X-ray diffraction techniques and the molecular structure has also been optimized at the B3LYP/6-31 G(d, p) level using density functional theory (DFT). The triazole ring exhibits dihedral angles of 41.61(15)º and 80.73(11)º with the phenyl rings. The molecules are linked principally by N–H···N hydrogen bonds involving the amino NH_2 group and a triazole N atom, forming C(5) chains which are further linked to give a two-dimensional network of molecules. The N–H···N hydrogen bonding is supported by C–H···N hydrogen bond and C–H···π interaction. Intermolecular N–H···N and C–H···N hydrogen bonds produce $R_2^2(9)$, $R_4^4(10)$ and $R_4^4(20)$ rings.

Keywords: crystal structure, chlorophenyl, triazole, hydrogen bonds

1 INTRODUCTION

1,2,4-Triazole and its derivatives have been used as starting materials for the synthesis of many heterocycles[1]. The triazole ring, having strong σ-donor and weak π-acceptor properties, potentially has two different coordination modes through three nitrogen donor atoms coordinating to the metal ions[2~5]. Recent interest in substituted 1,2,4-triazoles has arisen in part from their transition metal complexes with intriguing structures and specific magnetic properties[6, 7]. Many metal complexes containing substituted 1,2,4-triazole have potential applications in molecule-based memory devices, displays and optical switches due to their spin crossover properties[8, 9]. Apart from their chemical significance, 1,2,4-triazole derivatives have been found to be associated with diverse pharmacological properties, such as anti-inflammatory, antifungal and antiviral[10~12]. Some of them are also known to exhibit analgesic, anticonvulsant, tranquilizing, antidepressant, anxiolytic[13~16] or even antitumour activities[17] and are applied in therapy (e.g. Alprazolam, Estazolam, Triazolam and Adinazolam)[18]. In spite of the chemical and medicinal importance of this class of compounds, relatively fewer crystal structures of 1,2,4-triazole derivatives have been reported[19]. In this paper, we wish to report the

Received 25 September 2010; accepted 13 December 2010 (**CCDC 787642**)
① The authors acknowledge the Faculty of Arts and Sciences, Ondokuz Mayıs University, Turkey, for the use of the Stoe IPDSII diffractometer (purchased under grant No. F279 of the University Research Fund)
② Corresponding author. E-mail: onurs@omu.edu.tr

synthesis and crystal structure of the triazole compound, 4-amino-3-(*p*-chlorophenyl)-5-(*p*-methoxybenzyl)-4H-1,2,4-triazole, as well as the theoretical studies on it by using the DFT/B3LYP/6-31G(d, p) method.

2 EXPERIMENTAL

2. 1 Synthesis

For the preparation of the compound, acyl hydrazone (5 mmol) was added to the solution of hydrazine hydrat (10 mmol) in 1-propanol (50 mL) and the mixture was refluxed for 24 h. On cooling a percipitate was formed, and this product was filtered off and dried. The dry product was washed with benzene (20 mL). The insoluble part in benzene was recrystallized from 1-propanol to afford the pure compound. Recrystallization from ethyl acetate gave a white product (80% yield). Single crystals of the compound were obtained from ethyl acetate at room temperature by slow evaporation (m.p. 492～493 K). IR (Kbr, cm^{-1}): 3200 (NH_2), 3076 (Ar-CH), 2912 (CH), 1645 (C=N), 1450, 1380, 897. Anal. Calcd. for $C_{16}H_{15}ClN_4O$: C, 61.05; H, 4.80; N, 17.80%. Found: C, 60.95; H, 4.50; N, 17, 10%.

2. 2 Crystal structure determination

A colorless single crystal of the title compound, $C_{16}H_{15}ClN_4O$, was mounted on a glass fiber for data collection performed on a STOE IPDS II diffractometer with a graphite-monochromated Mo$K\alpha$ radiation at 296 K. The structure was solved by direct methods using SHELXS-97[20] and refined by full-matrix least-squares techniques on F^2 using SHELXL-97[20] from within the WINGX[21] suite of software. All non-hydrogen atoms were refined with anisotropic parameters. H atoms bonded to C atoms were included in their expected positions and allowed to ride, with C–H distances restrained to 0.93 and 0.97 Å. Amino H atoms were located in difference maps and refined freely. The refinement of the disordered O(1) and C(16) atoms were made anisotropically using PART and EADP restrictions. This disorder was modeled as two different orientations as A and B groups (hereafter A = O(1a), C(16a) and B = O(1b), C(16b)), seen in Fig. 1, with occupancy factors of 0.676(13) and 0.324(13), respectively. Molecular diagrams were created using ORTEP-III[22]. Geometric calculations were performed with PLATON[23]. The crystallographic data and other pertinent information are summarized in Table 1.

Table 1. Crystal Data and Refinement Parameters for Compound I

Empirical formula	$C_{16}H_{15}ClN_4O$
Formula weight (g/mol)	314.77
Crystal size (mm)	0.48 × 0.30 × 0.02
Crystal system	Monoclinic
Space group	$P2_1/c$
a (Å)	14.9217(9)
b (Å)	10.4885(11)
c (Å)	10.3178(7)
β (°)	102.795(5)
V (Å^3)	1574.7(2)
Z	4
Calculated density (g/cm^3)	1.328
λ(Mo$K\alpha$) (Å)	0.71073
μ(Mo$K\alpha$) (mm^{-1})	0.250
F(000)	656
θ range for data collection (°)	2.0 to 28.0
θ_{min}, θ_{max} (°)	2.39, 27.00
h, k and l ranges	$-19 \leqslant h \leqslant 19$, $-9 \leqslant k \leqslant 13$ $-13 \leqslant l \leqslant 13$
Reflections measured	9248
Independent reflections	3399

To be continued	
Observed reflection ($I > 2\sigma(I)$)	1380
R_{int}	0.1072
Final R* indices ($I > 2\sigma(I)$)	R = 0.0664, wR = 0.0831
$w = 1/[\sigma^2(F_o^2) + (aP)^2]$, where $P = (F_o^2 + 2F_c^2)/3$	a = 0.0148
Goodness-of-fit	1.014
$(\Delta/\sigma)_{max}$	0.001
Max./min. $\Delta\rho$ (e/Å^3)	0.206 and –0.209

* $R = \sum(||F_o| - |F_c||)/\sum|F_o|$, $wR = \{\sum w[(F_o^2 - F_c^2)^2]/\sum w[(F_o^2)^2]\}^{1/2}$

2. 3 Computational procedure

The geometry optimization of the molecule leading to energy minima was achieved using the B3LYP hybrid exchange-correlation functional with the 6-31G(d, p) basis set[24, 25]. The calculations started from the crystallographically achieved geometries of the molecule. All calculations in this work were carried out using the GAUSSIAN03W package[26]. The optimized molecular geometry, total molecular energy and dipole moment calculations were obtained from the computational process.

3 RESULTS AND DISCUSSION

Compound **I** consists of a 1,2,4-triazole ring with chlorophenyl, amino and methoxybenzyl substituents at the 3-, 4- and 5-positions, respectively (Fig. 1). Least-squares mean plane calculations for the triazole (N(1)/N(2)/C(8)/N(3)/C(7)) and phenyl rings (C(1)～C(6) and C(10)～C(15)) planes show that these are approximately planar, with respective maximum deviations of 0.0065(19) Å for C(8), 0.0154(27) Å for C(4) and 0.0021(26) Å for C(14). The triazole ring exhibits dihedral angles of 41.61(15)° and 80.73(11)° with the phenyl rings. The N(3)–N(4) bond length (Table 2) is similar to that in 4-amino-3,5-bis(4-pyridyl)-1,2,4-triazole (1.411(4) Å)[27], and the N(1)–N(2) bond is close to that in 3,6-bis(2-chlorophenyl)-1,4-dihydro-1,2,4,5-tetrazine (1.395(3) Å)[28]. The C(7)–N(1) and C(8)–N(2) distances are in good agreement with those found for the structures containing the 1,2,4-triazole ring[29, 30].

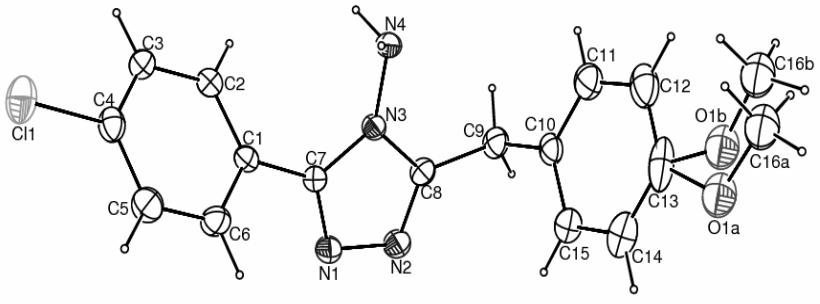

Fig. 1. A view of the molecule of I, showing the atom-numbering scheme. Displacement ellipsoids are drawn at the 30% probability

Table 2. Selected Bond Lengths (Å) and Bond Angles (°) for Compound I

Bond (Å)	X-ray	DFT/B3LYP
C(4)–Cl(1)	1.743(3)	1.756
N(3)–N(4)	1.406(3)	1.403
N(1)–N(2)	1.402(3)	1.379
C(7)–N(1)	1.306(4)	1.318
C(8)–N(2)	1.309(4)	1.314
C(8)–N(3)	1.361(3)	1.373
C(7)–N(3)	1.377(4)	1.385

Angle (°)	X-ray	DFT/B3LYP
C(3)–C(4)–Cl(1)	118.8(3)	119.5
C(6)–C(1)–C(7)	117.4(3)	117.8
C(8)–C(9)–C(10)	111.7(3)	113.1
N(3)–C(8)–C(9)–C(10)	78.1(4)	72.3

Molecules of **I** are linked into sheets by the combination of C–H···N and N–H···N hydrogen bonds (Table 4). Amino atom N(4) in the molecule at (*x*, *y*, *z*) acts as a hydrogen-bond donor, *via* atom H(4B), to atom N(1) in the molecule at (1–*x*, 1/2+*y*, 1/2–*z*), forming a C(5)[31] chain running parallel to the [010] direction. Similarly, atom C(2) in the molecule at (*x*, *y*, *z*) works as a hydrogen-bond donor, *via* atom H(2), to atom N(2) in the molecule at (1–*x*, 1/2+*y*, 1/2–*z*), generating a C(6) chain parallel to the [010] direction. The combination of the C(5) and C(6) chains generates a chain of edge-fused $R_2^2(9)$ rings running parallel to the [010] direction (Fig. 2). Amino atom N(4) in the molecule at (*x*, *y*, *z*) serves as a hydrogen-bond donor, *via* atom H(4A), to atom N(2) in the molecule at (*x*, 1/2–*y*, 1/2+*z*), forming a C(5) chain running parallel to the [001] direction. The combination of C(5) chains produced by intermolecular N–H···N hydrogen bonds generates a chain of edge-fused $R_4^4(10)$ and $R_4^4(20)$ rings parallel to the *bc* plane (Fig. 3).

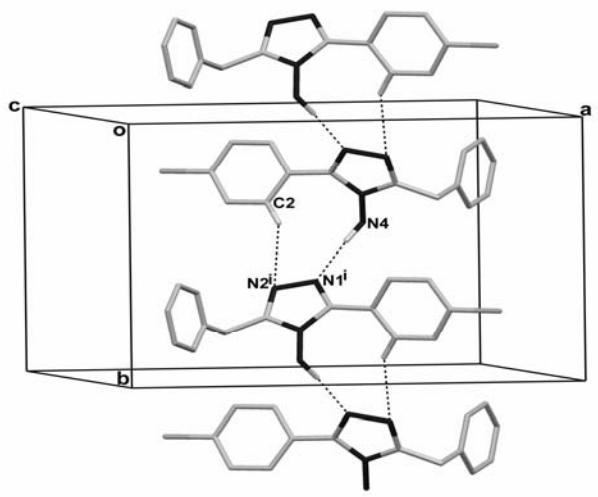

Fig. 2. Crystal structure of I, showing the formation of a $R_2^2(9)$ ring. For the sake of clarity, H and disordered atoms not involved in the motif shown have been omitted (Symmetry code as in Table 4)

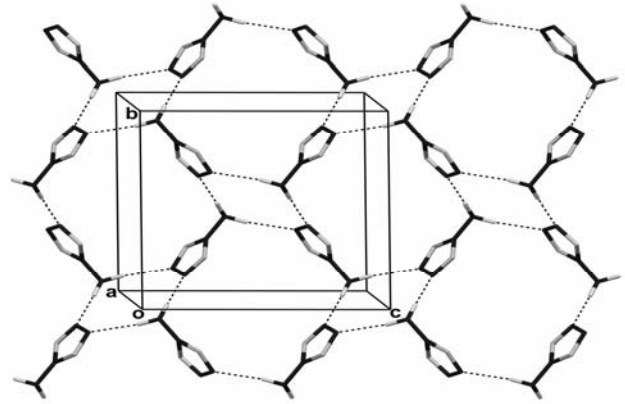

Fig. 3. Part of the crystal structure of I, showing the formation of a chain of edge-fused $R_4^4(10)$ and $R_4^4(20)$ rings. For clarity, H, C, O and Cl atoms not involved in the motif shown have been omitted

In the structure of **I**, there also exists a strong C–H···π interaction. Atom C(9) in the molecule at (x, y, z) acts as a hydrogen-bond donor to the C(10)~C(15) benzene ring in the molecule at (x, 1/2–y, –1/2+z), thus forming a chain running parallel to the [001] direction. Details of this interaction are given in Table 4. The combination of C–H···π interactions and N–H···N hydrogen bonds defines an $R_2^2(11)$ ring pattern (Fig. 4).

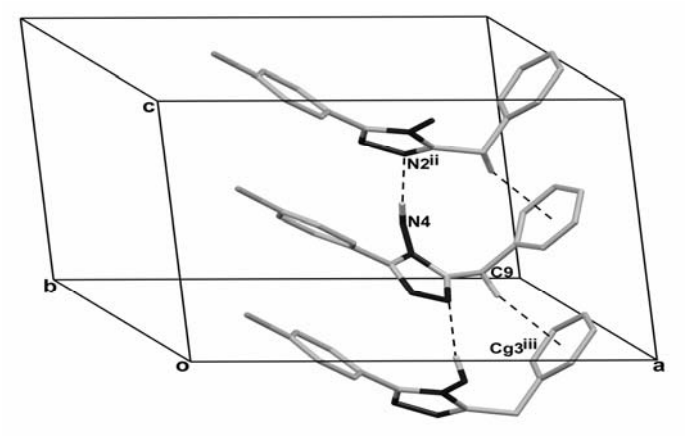

Fig. 4. Crystal structure of I, showing the formation of a chain along [001] generated by the C-H···π interactions. For clarity H and disordered atoms not involved in the motif shown have been omitted (Symmetry codes as in Table 4)

As seen from Table 2, the optimized bond lengths are slightly different from the experimental values. The biggest difference of the bond lengths between the experimental and predicted values is found at the N(1)–N(2) bond, with the different value being 0.023 Å for the B3LYP method. For the bond angles, the biggest difference is observed for C(8)–C(9)–C(10) and the different value is 1.4º. Similarly, the biggest difference occurs at the N(3)–C(8)–C(9)–C(10) torsion angle, with the different value to be 5.8º. According to the above comparisons, it can be deduced that, for the title compound, the biggest differences of the bond lengths, bond angles and torsion angles are mainly found in the groups involved in the hydrogen bonds, which can be easily understood *via* taking into account the intermolecular hydrogen bond interactions present in the crystal.

In the DFT/B3LYP calculations, the total energy of the optimized geometry and the dipole moment are obtained as -5.986×10^{-15} J and 6.1096 D for **I**. Mulliken charges were calculated by determining the electron population of each atom as defined by the basis sets. According to the calculated results for Mulliken atomic charge analysis, atoms O(1), N(3) and N(4), as expected, have larger negative charges relative to other atoms (Table 3).

Table 3. Mulliken Atomic Charges for Compound I

C(1)	0.095624	C(12)	–0.135112
C(2)	–0.122813	C(13)	0.346729
C(3)	–0.077255	C(14)	–0.113732
C(4)	–0.091439	C(15)	–0.122084
C(5)	–0.078576	C(16)	–0.077868
C(6)	–0.092153	N(1)	–0.367596
C(7)	0.433613	N(2)	–0.357679
C(8)	0.515555	N(3)	–0.444103
C(9)	–0.289689	N(4)	–0.439412
C(10)	0.104888	O(1)	–0.516875
C(11)	–0.146494	Cl(1)	–0.013729

Table 4. Hydrogen Bonds and C–H$\cdots\pi$ Interaction for Compound I (Å and °)

D–H···A	d(D–H)	d(H···A)	d(D···A)	<(DHA)
N(4)–H(4B)···N(1)#1	0.94(4)	2.10(4)	3.036(4)	176(3)
N(4)–H(4A)···N(2)#2	0.95(4)	2.10(4)	3.032(4)	168(4)
C(2)–H(2)···N(2)#1	0.93	2.58	3.411(5)	150
C(9)–H(9B)···Cg(3)#3	0.97	2.93	3.845(3)	158

Cg(3) is the centroid of the C(10)~C(15) ring. Symmetry codes: #1: 1–*x*, *y*+1/2, –*z*+1/2; #2: *x*, –*y*+1/2, *z*+1/2; #3: *x*, –*y*+1/2, *z*–1/2

Fig. 5 shows the distributions and energy levels of the HOMO-1, HOMO, LUMO and LUMO +1 orbitals computed at the DFT/B3LYP/6-31G(d,p) level for the title compound. Both the highest occupied molecular orbitals (HOMOs) and the lowest unoccupied molecular orbitals (LUMOs) are mainly localized on the rings, indicating that the HOMO-LUMO are mostly the π-antibonding type orbitals. The value of the energy separation between HOMO and LUMO is 4.713 eV, and this large energy gap indicates the title structure to be quite stable.

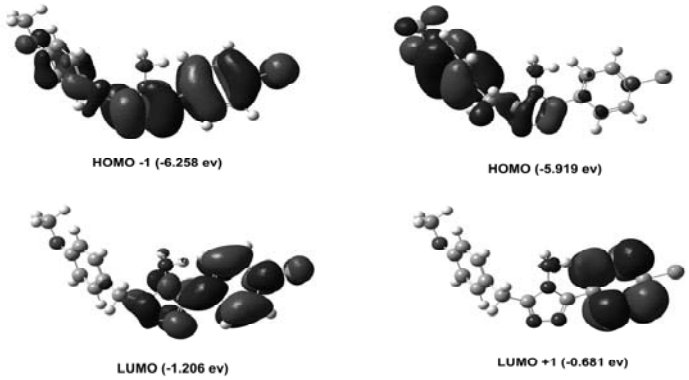

Fig. 5. Molecular orbital surfaces and energy levels given in parentheses for the HOMO -1, HOMO, LUMO, and LUMO +1 of I computed at the DFT/B3LYP/6-31G(d,p) level

REFERENCES

(1) Desenko, S. M. *Khim. Geterotsikl. Soedin. (Chem. Heterocycl. Comput.)* **1995**, pp. 2–24.

(2) Van Diemen, J. H.; Haasnoot, J. G.; Hage, R.; Reedijk, J.; Vos, J. G.; Wang, R. *Inorg. Chem*. **1991**, 30, 4038–4043.

(3) Ding, B.; Yi, L.; Zhu, L. N.; Cheng, P.; Liao, D. Z. *Journal of Coordination Chemistry* **2004**, 57, 9–16.

(4) Yi, L.; Ding, B.; Zhao, B.; Cheng, P.; Liao, D. Z.; Yan, S. P.; Jiang, Z. H. *Inorg. Chem.* **2004**, 43, 33–43.

(5) Ren, P.; Ding, B.; Shi, W.; Wang, Y.; Lu, T.; Cheng, P. *Inorganica Chimica Acta* **2006,** 359, 3824–3830.

(6) Zhou, J. H.; Cheng, R. M.; Song, Y.; Li, Y. Z.; Yu, Z.; Chen, X. T.; Xue, Z. L.; You, X. Z. *Inorg. Chem.* **2005**, 44, 8011–8022.

(7) Zhou, J. Z.; Cheng, R. M.; Song, Y.; Li, Y. Z.; Yu, Z.; Chen, X. T.; You, X. Z. *Polyhedron* **2006**, 25, 2426–2432.

(8) Garcia, Y.; van Koningsbruggen, P. J.; Codjovi, E.; Lapouyade, R.; Kahn, O.; Rabardel, L. *J. Mater. Chem.* **1997**, 7, 857–858.

(9) Kahn, O.; Martinez, C. J. *Science* **1998**, 279, 44–48.

(10) Massa, S.; Di Santo, R.; Retico, A.; Artico, M.; Simonetti, N.; Fabrizi, G.; Lamba, D. *Eur. J. Med. Chem.* **1992**, 27, 495–502.

(11) Mahomed, E. A.; El-Deen, I. M.; Ismail, M. M.; Mahomed, S. M. *Indian J. Chem. Sect. B* **1993**, 32, 933–937.

(12) Mullican, M. D.; Wilson, M. W.; Connor, D. T.; Kostlan, C. R.; Schrier, D. J.; Dyer, R. D. *J. Med. Chem.* **1993**, 36, 1090–1099.

(13) Bradbury, R. H.; Rivett, J. E. *J. Med. Chem.* **1991**, 34, 151–157.

(14) Sughen, J. K.; Yoloye, T. *Pharm. Acta Helv.* **1978**, 58, 64–68.

(15) Stillings, M. R.; Welbourn, A.; Walter, D. S. *J. Med. Chem.* **1986**, 29, 2280–2284.

(16) Kane, J. M.; Dudley, M. W.; Sorensen, S. M.; Miller, F. P. *J. Med. Chem.* **1988**, 31, 1253–1258.

(17) Hatheway, G. J.; Hansch, C.; Kim, K. H.; Milstein, S. R.; Schmidt, C. L.; Smith, R. N.; Quinn, F. R. *J. Med. Chem.* **1978**, 21, 563–567.

(18) Budavari, S.; O'Neil, M. J.; Smith, A.; Heckelman, P. E.; Kinnearty, J. F. *Editors* **1996**, The Merck Index, 12th Ed., Entries 159, 320, 3744 and 9734.

New Jersey: Merck and Co. Inc.

(19) Allen, F. H. *Cambridge Structural Database, Version 5.27. (November, 2005). Acta Cryst.* **2002**, B58, 380–388.

(20) Sheldrick, G. M. *Acta Cryst*. **2008**, A64, 112–122.

(21) Farrugia, L. J. *J. Apply. Cryst.* **1999**, 32, 837–838.

(22) Farrugia, L. J. *Appl. Crystallogr.* **1997**, 30, 565.

(23) Spek, A. L. *PLATON – A Multipurpose Crystallographic Tool*, Utrecht, Utrecht University, The Netherlands **2005**.

(24) Lee, C.; Yang, W.; Parr, R. G. *Phys. Rev. B* **1988**, 37, 785–789.

(25) Becke, A. D. *J. Chem. Phys.* **1993**, 98, 5648–5652.

(26) Frisch, M. J.; Trucks, G. W.; Schlegel, H. B.; Scuseria, G. E.; Robb, M. A.; Cheeseman, J. R.; Montgomery, J. A.; Vreven, Jr. T.; Kudin, K. N.; Burant, J. C.; Millam, J. M.; Iyengar, S. S.; Tomasi, J.; Barone, V.; Mennucci, B.; Cossi, M.; Scalmani, G.; Rega, N.; Petersson, G. A.; Nakatsuji, H.; Hada, M.; Ehara, M.; Toyota, K.; Fukuda, R.; Hasegawa, J.; Ishida, M.; Nakajima, T.; Honda, Y.; Kitao, O.; Nakai, H.; Klene, M.; Li, X.; Knox, J. E.; Hratchian, H. P.; Cross, J. B.; Adamo, C.; Jaramillo, J.; Gomperts, R.; Stratmann, R. E.; Yazyev, O.; Austin, A. J.; Cammi, R.; Pomelli, C.; Ochterski, J. W.; Ayala, P. Y.; Morokuma, K.; Voth, G. A.; Salvador, P.; Dannenberg, J. J.; Zakrzewski, V. G.; Dapprich, S.; Daniels, A. D.; Strain, M. C.; Farkas, O.; Malick, D. K.; Rabuck, A. D.; Raghavachari, K.; Foresman, J. B.; Ortiz, J. V.; Cui, Q.; Baboul, A. G.; Clifford, S.; Cioslowski, J.; Stefanov, B. B.; Liu, G.; Liashenko, A.; Piskorz, P.; Komaromi, I.; Martin, R. L.; Fox, D. J.; Keith, T.; Al-Laham, M. A.; Peng, C. Y.; Nanayakkara, A.; Challacombe, M.; Gill, P. M. W.; Johnson, B.; Chen, W.; Wong, M. W.; Gonzalez, C.; Pople, J. A. *Gaussian 03, Revision E.01*, Gaussian, Inc., Pittsburgh, P. A. **2003**.

(27) Guo, Y. M.; Du, M. *Acta Cryst.* **2002**, E58, o966–o968.

(28) Zachara, J.; Madura, I.; Wılostowski, M. *Acta Cryst.* **2004**, C60, o57–o59.

(29) Özbey, S.; Ulusoy, N.; Kendi, E. *Acta Cryst.* **2000**, C56, 222–224.

(30) Zhu, D. R.; Xu, Y.; Zhang, Y.; Wang, T. W.; You, X. Z. *Acta Cryst.* **2000**, C56, 895–896.

(31) Bernstein, J.; Davis, R. E.; Shimoni, L.; Chang. N. L. *Angew Chem. Int. Ed. Engl.* **1995**, 34, 1555–1573.